Pulsed Pyroelectric Crystal-Powered Gamma Source

A.X. Chen[1], A.J. Antolak, K.-N Leung[2], D.H. Morse, T.N. Raber
Sandia National Laboratories, Livermore, CA 94550

Abstract

A compact pulsed gamma generator is being developed to replace radiological sources used in commercial, industrial and medical applications. Mono-energetic gammas are produced in the 0.4 - 1.0 MeV energy range using nuclear reactions such as $^{9}Be(D, n\gamma)^{10}B$. The gamma generator employs a RF-driven inductively coupled plasma ion source to produce deuterium ion current densities up to 2 mA/mm^2 and ampere-level current pulses can be attained by utilizing an array extraction grid. The extracted deuterium ions are accelerated to approximately 300 keV via a compact stacked pyroelectric crystal system and then bombard the beryllium target to generate gammas. The resulting microsecond pulse of gammas is equivalent to a radiological source with curie-level activity.

1. Background

Gamma emitting radiological sources offer a simple and compact solution for producing mono-energetic photons with energies of approximately a megavolt. These sources are widely used in commercial, industrial, and medical applications such as gamma-density logging of boreholes where a ^{137}Cs source is used in conjunction with NaI gamma detectors to determine the formation density [1]. When used in tandem with a neutron porosity log [2], the combined data can provide petroleum companies with valuable information about where the oil deposits are located. In industry, ^{192}Ir sources are commonly used for non-destructive testing and imaging

[1]Corresponding author and also affiliated with Department of Mechanical Engineering at University of California-Berkeley
[2]Also affiliated with Department of Nuclear Engineering at University of California-Berkeley

of thick materials [3]. Cobalt-60 sources have found widespread use in medical radiotherapy applications such as the gamma knife which is a non-surgical tool for treating various forms of brain tumors [4].

The main challenge for gamma source replacement lies in matching both the energy spectra and output flux of radiological sources in a reasonably compact size. While there has been substantial work in developing megavolt bremsstrahlung photon sources using linear accelerators [5], no compact electronic source exists that produces mono-energetic gammas. This paper describes the development of a compact gamma source based on the $^{9}Be(d,n\gamma)^{10}B$ nuclear reaction to generate megavolt-energy photons with curie-equivalent activity level.

2. Nuclear Reactions to Produce Megavolt-Energy Gammas

The $^{9}Be(D,n\gamma)^{10}B$ nuclear reaction produces gamma rays in the 0.4 – 1.5 MeV range [6] and also neutrons in the 1.0 – 4.3 MeV range. Figure 1a shows the $^{9}Be(D,n\gamma)^{10}B$ gamma spectrum acquired with a NaI detector having peaks at 410 keV, 718 keV, 1.02 MeV, and 1.44 MeV. The neutrons produced in the reaction can be converted to 480 keV gammas via the $^{10}B(n,\alpha\gamma)^{7}Li$ reaction if a pure photon source is needed in an application. For incident 300 keV deuterium ions, the 718 keV gamma yield (Fig. 1b) is about $10^{11}\gamma$/s with a 1 ampere current pulse which is on the order of a curie-level activity radiological source. Above 300 keV operating voltage, the reaction cross section continues to increase but it does so at a much slower rate and, from a practical perspective, high voltage breakdown also becomes an issue in an electronic device.

The $^{6}Li(D,n\gamma)^{7}Be$ nuclear reaction produces two gamma rays at 431 and 478 keV [6]. The cross-section for this reaction is slightly higher than the D-^{9}Be reaction, which would

provide somewhat higher gamma intensities for a given beam power. In addition, the two gammas are nearly identical in energy, which provides operational functionality as a single gamma with double the yield. As mentioned above, if a pure photon source is needed, the neutrons produced in the reaction can be converted to 480 keV gammas via the $^{10}B(n,\alpha\gamma)^{7}Li$ reaction. The cross section for this reaction is similar to the D-^{9}Be reaction above in terms of flattening out above 300 keV. As a result, the gamma source under development is designed to operate at 300 keV.

3. Gamma Source Design

The three main components of the present gamma source are (1) ion source and extraction system, (2) gamma production target and (3) ion acceleration system. Ions are generated in an RF-driven inductive discharge plasma and extracted through a small aperture in a specially designed mechanical shutter for pulsing the beam. The pulse of ions is then accelerated to high voltage using a compact pyroelectric crystal powering system [7]and bombard a beryllium target to produce gammas. The following sections describe these components in detail.

3.1 Ion Source and Extraction System

Ampere-level deuterium ion beam current can be achieved in an RF inductive discharge plasma source where extracted current densities up to 2 mA/mm^2 have been previously demonstrated [8]. As seen in Fig. 2, the multi-cusp magnetic configuration provides a uniform plasma extraction area of up to 5 inch diameter allowing high current to be extracted using an array of multiple apertures. The RF source can also generate negative ions for D^- extraction to exploit both the heating and cooling phases of the pyroelectric crystal acceleration system, essentially doubling the duty factor of the gamma source.

One drawback with an RF source is the high gas load needed for maintaining optimal plasma characteristics. Generally, a pressure of $>10^{-2}$ Torr is needed for stable operation in the inductive mode [9]. In contrast, the acceleration chamber requires high vacuum ($<10^{-5}$ Torr) to hold off 300 kV which usually means a very large turbo-pump is needed to provide vacuum isolation. This problem was overcome in the gamma source design by implementing a fast mechanical shutter system which enables both vacuum isolation and pulsed-mode operation [10]. With this system, a one-millisecond FWHM beam pulse from a single aperture was demonstrated and vacuum pressures in the acceleration chamber was improved an order of magnitude with the shutter in place. The development of a multi-aperture shutter is currently underway to provide high current from many ion beamlets to generate a high yield of gammas at the target.

3.2 Gamma Production Target

Solid beryllium has very high thermal conductivity and melting point which are critical properties for high power applications such as the target material in the gamma source where an instantaneous power of ~300 kW is required during pulsed operation. Typical limits for forced convective boiling can provide a maximum heat flux removal of 2.5 kW/cm^2. Therefore, a beryllium target needs to be at least 5 inches in diameter for stable operation and, as mentioned above, the multi-cusp RF ion source is capable of providing uniform beam current over this area.

Preparing a target for the D-^{6}Li reaction presents a greater challenge compared to beryllium. Because the natural abundance of ^{6}Li is 7.5%, isotope enrichment must be done to produce a target containing a high percentage of ^{6}Li. Furthermore, most lithium-containing compounds such as LiF and Li_2CO_3 are insulators which must be fabricated into thin films for use as a gamma production target. Such a target is impractical considering the thermal and sputtering damage when servicing in a high power gamma source. Solid ^{6}Li metal can be used

as a thick target, but its low melting point makes it unsuitable for use as a high power gamma production target.

3.3 High voltage pyroelectric driven powering system

Pyroelectric crystals, such as $LiTaO_3$, were previously demonstrated to achieve high voltages in a compact size [11,12,13,14]. Voltage is developed between the polar faces of the crystal and is linearly dependent on the temperature change as given by

$$\Delta V = \left(\frac{\gamma}{\varepsilon} \cdot L\right)(\Delta T)$$

where ΔV is the voltage difference across the crystal, γ is the pyroelectric coefficient, ε is the electric permittivity, L is the length of the crystal, and ΔT is the change in temperature. Using a 30 mm diameter x 30 mm long $LiTaO_3$ crystal in high vacuum ($<10^{-5}$ Torr), negative voltages up to 125 kV were generated by heating the crystal approximately 10^{o}C on one end using a thermoelectric device. During these experiments, it was found that the peak voltage was limited by voltage breakdown through surface discharge along the crystal (Fig. 4). With a 30 mm diameter x 10 mm long crystal, the maximum voltage was only 75 kV when heated by 16^{o}C, again limited by arcing across the surface. In addition, the heating rate must be restricted to no more than ~0.03^{o}C/s to maintain temperature uniformity and prevent thermal stress damage to the crystal [12].

More uniform and fast heating/cooling can be done with thin crystals. For example, one millimeter thick crystals allow at least an order of magnitude higher heating rate without sacrificing temperature uniformity, resulting in higher yields and more stable operation. To take advantage of these features, a high voltage heating/cooling module was designed and fabricated to accommodate a thin 50 mm diameter x 1 mm long (thick) crystal (Fig. 6). The crystal was

heated with an average heating rate of 1.4°C/s from 27°C to 89°C before breakdown occurred across the crystal. The experimental limit due to the coercive field of $LiTaO_3$ crystals of 22 kV/mm [15] was demonstrated in this module. In normal operations, the crystals are charged up by heating (cooling) in a dielectric fluid to reach electric fields of ~15 kV/mm [16]. The dielectric fluid was chosen for its high boiling point which helps to reduce vapor formation during heating. The capacitance of a single crystal module was measured to be ~1 nF. Table 1 summarizes the electrical characteristics of the three different size crystals that were tested. Notice that for the 1 mm long crystal, the sustained electric field is 3 times higher than the 10 mm long crystal and over 5 times higher than the 30 mm long crystal.

As discussed earlier, the pyroelectric crystal powering system is operated at ~300 kV for gamma production. However, as the voltage increases above 100 kV, field emission and corona losses become increasingly significant [12]. Because the pyroelectric powering system is a charge limited device, the voltage will stop increasing when the charge generation rate equals the charge loss rate, putting an upper bound on the highest obtainable voltage. One way to overcome this barrier is to operate the crystals in pulsed mode by stacking the crystals into a series configuration for the duration of no more than a few microseconds, thus minimizing the charge loss. Figure 7 shows the stacking of four 1 mm thick crystals that initially each charged to a voltage of at least 15 kV. At the high voltage terminal, the arc distance in air to ground confirmed that a final output of greater than 60 kV was achieved. To achieve 300 kV, a system of twenty pyroelectric crystal modules will be stacked in a special mounting device that is being developed to isolate the thermoelectric heater power from the high voltage.

4. Conclusion

The design of a compact mono-energetic electronic gamma source for replacing megavolt-energy radiological gamma sources is described. In particular, the D-Be reaction produces gammas with energies similar to the gamma emissions of Co-60, Cs-137, and Ir-192. Because of the energy similarity, data interpretations between the electronic and radiological sources would require little effort to migrate from one source to the other. The main challenge is matching the flux of a radiological source while keeping the overall system size compact. Using an RF ion source, it is possible to provide sufficient beam current for generating pulses of curie-level gammas. Stacking pyroelectric crystals in series enables one to reach both the high voltages needed for the gamma generator as well as producing pulsed gamma bursts. The latter feature could be very useful for imaging and applications requiring the detection of delayed responses from gamma pulses.

5. Acknowledgements

This work was funded by DOE/NA-22 Office of Nonproliferation Research and Development. The authors would like to thank Dr. Vincent Tang for providing the 3cm x 3cm $LiTaO_3$ crystal, dielectric fluid, and for technical discussions. Sandia National Laboratories is a multi-program laboratory managed and operated by Sandia Corporation, a wholly owned subsidiary of Lockheed Martin Corporation, for the U.S. Department of Energy's National Nuclear Security Administration under contract DE-AC04-94AL85000.

6. References

[1] D.V. Ellis and J.M. Singer, *Well Logging for Earth Scientists*, 2nd ed.: Springer, 2008.

[2] A. X. Chen, A. J. Antolak, and K.-N. Leung, "Electronic Neutron Sources for Compensated Porosity Well Logging," *Nuclear Instruments and Methods in Physics Research Section A*, Vol. 684, pp. 52-56, 2012.

[3] R.S. Holt, M.J. Cooper, and D.F. Jackson, "Gamma-ray scattering techniques for non-destructive testing and imaging," *Nuclear Instruments and Methods in Physics Research 221*, Vol. 221, pp. 98-104, 1984.

[4] FAQ About Gamma Knife. (http://neurosurgery.ucsf.edu/index.php/radiosurgery_gammaknife_FAQ.html)

[5] S. Boucher, R. Agustsson, L. Faillace, P. Frigola, A. Murokh, M. Ruelas, S. Storms, X. Ding, "Compact, Inexpensive X-Band LINACS as Radioactive Isotope Source Replacement," in *IPAC*, 2012, pp. 4136-4138.

[6] F.E. Cecil, R.F. Fahlsing, and R.A. Nelson, "Total cross-section measurements for the production ofnuclear gamma rays from light nuclei by low energy deuterons," *Nuclear Physics A*, Vol. 376, pp. 379-388, 1982.

[7] A.X. Chen, A.J. Antolak, K.-N. Leung, T.N. Raber, and D.H. Morse, "Compact Electronic Gamma Source for Radiotherapy," in *CAARI 2010*, 2011, pp. 413-417.

[8] K.N. Leung, G.J. DeVries, W.F. DiVergilio, R.W. Hamm, C.A. Hauck, W.B. Kunkel, D.S. McDonald, M.D. William, "RF Driven Multicusp H- Ion Source," *Review of Scientific Instruments*, Vol. 62, pp. 100-104, 1990.

[9] Ka-Ngo Leung, "The application and status of the radio frequency driven multi-cusp ion

source (invited)," *Review of Scientific Instruments*, Vol. 71, pp. 1064-1068, 2000.

[10] A.X. Chen, A.J. Antolak, K.-N. Leung, D.H. Morse, and T.N. Raber, "Fast mechanical shutter for pulsed ion beam generation," *Nuclear Instruments and Methods in Physics Research Section A*, Vol. 670, pp. 45-48, 2012.

[11] B. Naranjo, J.K. Gimzewski, and S. Putterman, "Observation of nuclear fusion driven by a pyroelectric crystal," *Nature*, Vol. 434, pp. 1115-1117, 2005.

[12] V. Tang,G. Meyer, S. Falabella, G. Guethlein, S. Sampayan, P. Kerr, B. Rusnak, J.D. Morse, "Intense pulsed neutron emission from a compact pyroelectric driven accelerator,"*Journal of Applied Physics*, Vol. 105, 26103, 2009.

[13] J.A. Geuther and Y. Danon, "High-energy x-ray production with pyroelectric crystals," *Journal of Applied Physics*, Vol. 97, 104916, 2005.

[14] W. Tornow, S.M. Shafroth, and J.D. Brownridge, "Evidence of neutron production in deuterium gas with a pyroelectric crystal without tip," *Journal of Applied Physics*, Vol. 104, 034905, no. 3, 2008.

[15] M. Unterberger, E. Born, G. Kovacs, E. Riha, and T. Holzheu, "Electrode Enhanced Pyroelectric Domain Reversal in Ferroelectric Crystals," in *ISAF 2000*, 2000, pp. 779-782.

[16] 3M Fluorinert Electronic Liquid FC-70. (http://multimedia.3m.com/mws/mediawebserver?mwsId=66666UF6EVsSyXTtnxTE5Xz6EVtQEVs6EVs6EVs6E666666--&fn=prodinfo_FC70.pdf)

1

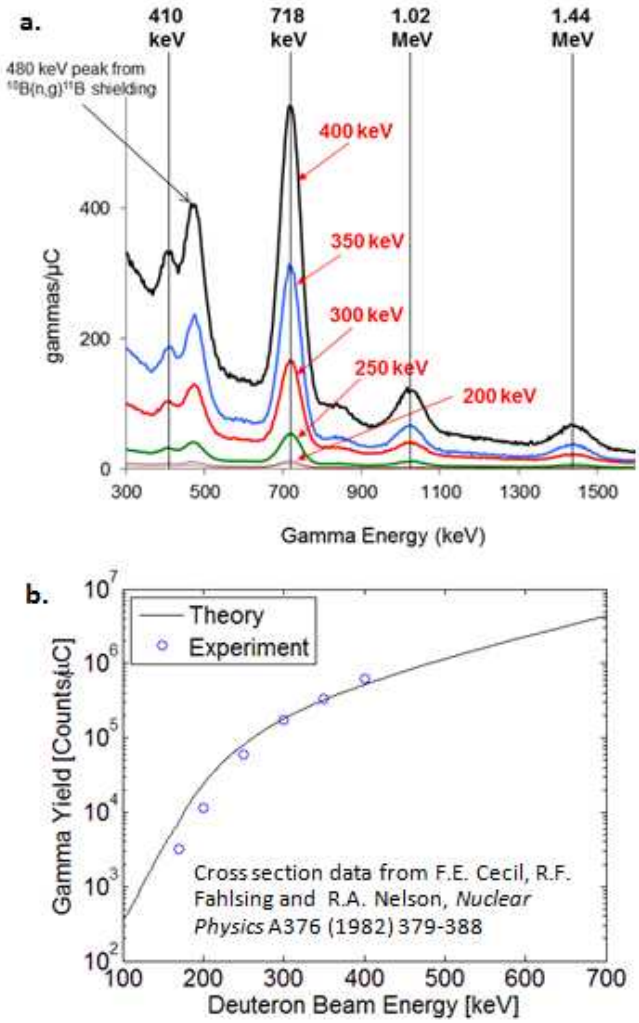

FIGURE 1. (a) Gamma energy spectra of the D-^{9}Be reaction at different incident deuteron beam energies. (b) Gamma yield as a function of the incident deuteron energy.

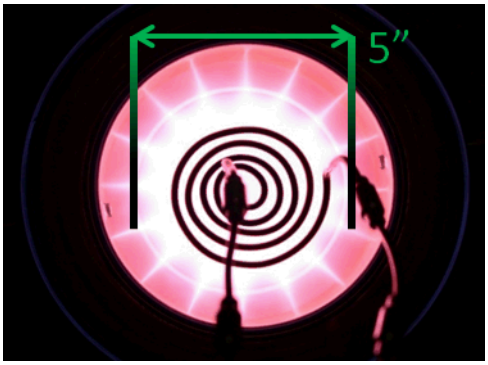

FIGURE 2. The RF plasma source operating with hydrogen in the inductive discharge mode. Multi-cusp magnetic fields create a region (5” diameter) of uniform plasma for extraction.

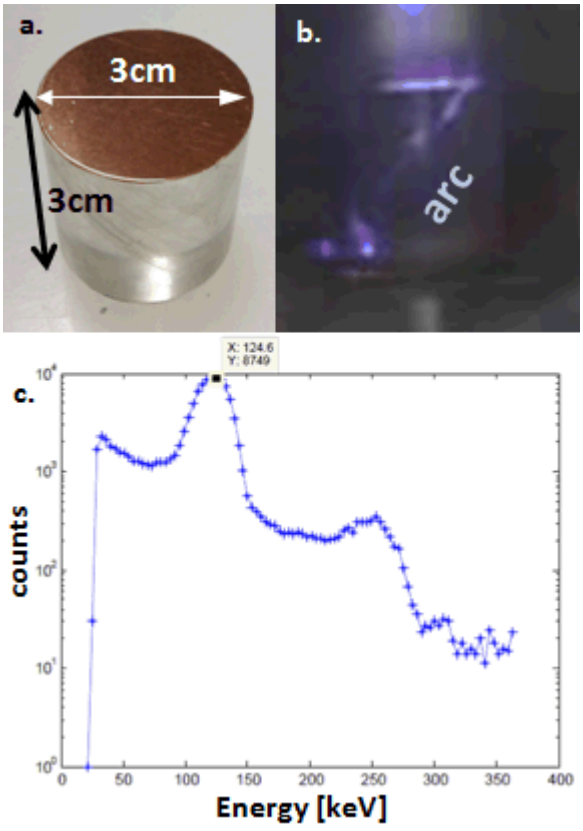

FIGURE3. (a) 30 mm diameter x 30 mm $LiTaO_3$ crystal. (b) Arc discharge along the crystal surface in high vacuum. (c) Measured energy spectrum of the field emission electrons using a silicon surface barrier detector.

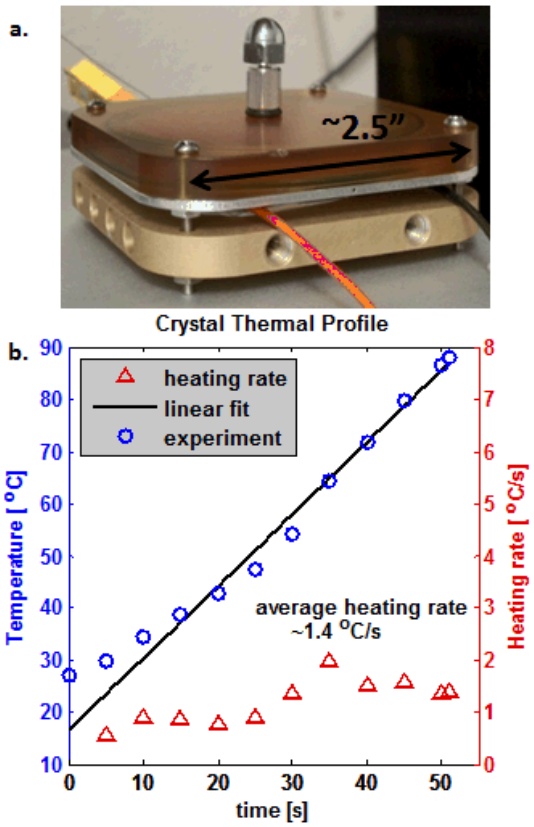

FIGURE4. (a) Photo of the single crystal module with thermoelectric device and sealed dielectric fluid to suppress arcing and vapor formation. (b) Temperature and heating rate measurements of a single crystal module. Heating rate is increased by more than one order of magnitude compared to the longer crystal cases.

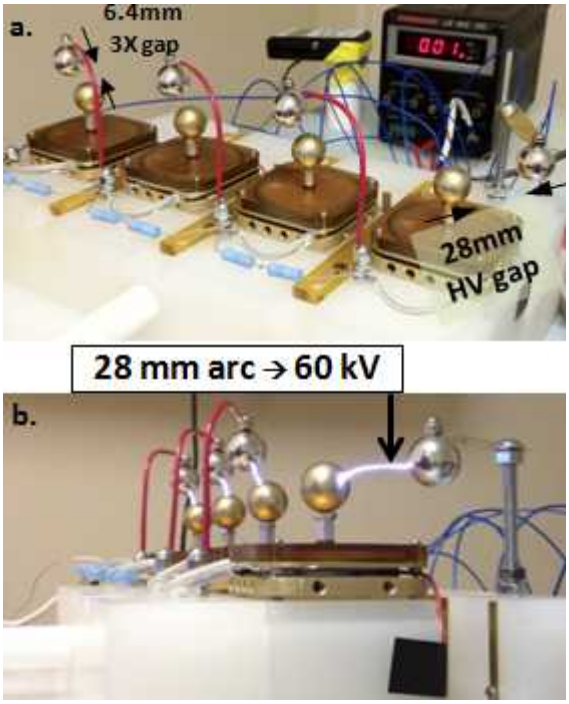

FIGURE5. (a) Stacking configuration for a 4-crystal system. All modules are simultaneously heated to ~15kV. (b) During the pulse discharge, the four crystals are instantaneously connected in series to obtain a voltage of ~60kV.

TABLE 1. Measured values for the electric field, average temperature difference, and volume specific energy storage of different length $LiTaO_3$ crystals.

Data for different length crystals

Length (mm)	E-field (kV/mm)	Average ΔT (K)	Energy (kJ/m³)
1	22	62	123
10	7.5	15.7	11.2
30	4.2	8.8	3.5